

<sup>1</sup> **Irrigation impacts on California's climate with the**  
<sup>2</sup> **variable-resolution CESM**

Xingying Huang,<sup>1</sup> Paul A. Ullrich,<sup>1</sup>

---

0

Corresponding author: Xingying Huang, Department of Land, Air and Water Resources,  
University of California Davis, Davis, CA 95616, USA. (xyhuang@ucdavis.edu)

<sup>10</sup>Department of Land, Air and Water  
Resources, University of California, Davis

**Abstract.**

The variable-resolution capability within the Community Earth System Model (VR-CESM) is applied to understand the impact of irrigation on the regional climate of California. Irrigation is an important contributor to the regional climate of heavily irrigated regions, and within the U.S. there are few regions that are as heavily irrigated as California's Central Valley, responsible for 25% of domestic agricultural products. A flexible irrigation scheme with relatively realistic estimates of agricultural water use is employed. The impact of irrigation on mean climatology and heat extremes is investigated over the 26 year period 1980-2005 using a relatively fine grid resolution of  $0.25^\circ$  ( $\sim 28$  km). Three simulations are performed, including an unirrigated control run and two irrigation-enabled runs, with results compared to gridded observations and weather station datasets. During the summer months (when irrigation peaks), the cooling effect caused by irrigation to the daily maximum near-surface temperature field ( $T_{\max}$ ) is approximately 1.1 K. Under irrigation, latent heat flux increased by  $\sim 61\%$  during the daytime as a result of increased surface evaporation; specific humidity increased by about 12%; heat stress was reduced by 22% and the average soil moisture showed a small magnitude ( $\sim 4.4\%$ ) but statistically significant increase. Compared with observations, irrigation improved the frequency distribution of  $T_{\max}$ , and both length and frequency of hot spells were better represented with irrigation enabled. Consequently, we argue that high-resolution simulations of regional climate in CESM, particularly over heavily irrigated regions, should

26 likely enable the irrigation parameterization to better represent local tem-  
27 perature statistics.

## 1. Introduction

Over the past century, human activity has had a clear impact on global and regional climate, largely through indirect effects associated with increasing greenhouse gases [?], but also as a result of land cover changes, particularly deforestation, agriculture and urbanization [Bonan, 1997; Pielke *et al.*, 2002; Kueppers *et al.*, 2008]. Conversion of the natural land cover to cropland features prominently in this change, which is accompanied by modified albedo and differences in both sensible and latent heat fluxes [Foley *et al.*, 2003]. Besides affecting energy balance, land management also impacts the climate system by modifying the carbon and water cycles, which are driven in part by cropping length and irrigation strategy [Lobell *et al.*, 2006]. The pronounced cooling effect of irrigation, especially over regions where irrigation is extensive, has been emphasized by previous studies [Kueppers *et al.*, 2007; Lobell and Bonfils, 2008].

California is the most irrigated state in the U.S., and most of California's irrigated cropland is distributed over the Central Valley (CV), which is responsible for 25% of domestic agricultural products [Wilkinson *et al.*, 2002]. The CV extends 600 km between its northernmost and southernmost point and is between 60-100km in width. It features a vast agricultural industry that has adapted to an extremely dry growing season under Mediterranean climate through the adoption of extensive irrigation practices. The USGS reported that in the year 2000, approximately 42 km<sup>3</sup> of water was used over ~41,000 km<sup>2</sup> of irrigated area within California [Döll and Siebert, 2002; Famiglietti *et al.*, 2011]. Bonfils and Lobell [2007] found that irrigation over CV has decreased summertime maximum temperature by ~2-3 K in heavily-irrigated areas compared with nearby non-irrigated areas,

based on long-term temperature records, although these impacts had a negligible effect on nighttime temperatures. Similar impacts have also been demonstrated in Nebraska's irrigated areas by *Mahmood et al.* [2006].

However, irrigation effects are usually ignored in climate models for several reasons: irrigation usually occurs over a relatively small area ( $\sim 2\%$  of global land surface) and produces a seemingly negligible cooling effect compared to global greenhouse warming [*Boucher et al.*, 2004]. Nonetheless, with the increasing need for more accurate regional climate studies for formulating climate adaptation and mitigation strategies, irrigation is a potentially important factor in regulating regional climate patterns. Studies have typically addressed the climatic effects of irrigation in limited-area models (LAMs) [*Snyder et al.*, 2006; *Kueppers et al.*, 2007], which in the context of climate modeling are typically referred to as regional climate models (RCMs). In these studies, irrigation was modeled by accounting for the amount of irrigated water needed and the area of cropland where irrigation is applied. Using a multi-model ensemble of RCM simulations, *Kueppers et al.* [2008] found that the behavior of RCMs varied in representing effects of irrigation on regional climate, depending on each model's physics, as well as on irrigation configurations.

Although global climate models (GCMs) rarely account for irrigation, it is nonetheless meaningful to understand to what extent irrigation may affect the global climate patterns [*Sacks et al.*, 2009]. *Lobell et al.* [2006] coupled the community atmosphere model (CAM) 3.0 to the community land model (CLM) 3.0 at  $\sim 2\text{-}2.5^\circ$  horizontal grid spacing to model irrigation by fixing soil moisture at saturation during the growing season in all croplands. Although this approach likely overcompensated for total added water, it was found that global irrigation led to a global land surface cooling of 1.3 K, and regional cooling of up

to 8 K. *Lo and Famiglietti* [2013] used CAM 3.5 along with CLM 3.5 at  $\sim 1.4^\circ$  horizontal resolution, and showed that the increase in evapotranspiration and water vapor due to irrigation significantly impacts the atmospheric circulation in the southwestern United States by strengthening the regional hydrological cycle [delete this?].

The aforementioned studies that addressed the impact of irrigation either used RCMs or coarse-resolution GCMs, along with different irrigation schemes. In order to model regional climate over the CV, relatively fine horizontal resolution is needed to more accurately represent microclimates, land-use, small-scale dynamical features and corresponding interactions [Leung et al., 2003; Rauscher et al., 2010]. In this paper, we use the recently developed variable-resolution option in Community Earth System Model (VR-CESM) to study the impact of irrigation on regional climate over the CV, with a more flexible irrigation scheme with relatively realistic estimates of regional agricultural water use (as will be described in Section 2). Variable-resolution GCMs (VRGCMs) such as VR-CESM use a relatively coarse global model with enhanced resolution over a specific region [Staniforth and Mitchell, 1978; Fox-Rabinovitz et al., 1997].

Compared with RCMs, a key advantage of VRGCMs is that they use a single, unified modeling framework, rather than a separate GCM and RCM with potentially inconsistent dynamics and physics parameterizations and lack of two-way interactions at the nest boundary [Laprise et al., 2008]. When compared to uniform-resolution global models, VRGCMs provide a cost-effective approach for reaching high resolutions over a region of interest – the regional simulations in this study at  $0.25^\circ$  ( $\sim 28$  km) resolution represent a reduction in required computation of approximately 10 times over a global uniform simulation with resolution at  $0.25^\circ$ . VR-CESM has been demonstrated to be effective for

regional climate studies and applications at a reduced computational cost compared to uniform GCMs [Zarzycki *et al.*, 2015; Rhoades *et al.*, 2015; ?]. In particular, this study is one of the first to use variable resolution for assessing the impact of a physical parameterization at high-resolution in a global Earth-system model. The central hypothesis of this paper is that irrigation in the CV of California is an important contributor to the region’s surface energy budget and must be accounted for in order to properly simulate temperature statistics, tested by a control (non-irrigated) and two irrigated 26-year simulations in VR-CESM.

This work builds on a number of previous modeling studies that have explored the importance of irrigation in controlling the climate over the CV region in the following ways: (1) it employs relatively high resolution ( $\sim 28$  km) covering the western U.S. over long-term period (from year 1980-01-01 to 2005-12-31); (2) it uses a more realistic irrigation parameterization embedded in CLM 4.0 coupled in CESM 1.2.0 rather than experimentally fixed irrigated water as in many previous studies (*i.e.* Lobell *et al.* [2006]; Lo and Famiglietti [2013]); (3) it uses a variable-resolution global climate model (rather than the low-resolution global or limited area models forced by reanalysis dataset or GCM output that have been previously used); and (4) it explores a more comprehensive array of impacts of irrigation on the regional climate, focusing on temperature statistics, including extreme heat episodes. We conclude that the irrigation parameterization in CESM is effective at addressing a bias in daily maximum temperatures and heatwave statistics in California’s CV, and is necessary in order to accurately capture temperature statistics in heavily irrigated regions at high model resolution.

This paper is organized as follows: Section 2 describes the model setup, employed datasets and methodology. In section 3, simulation results are provided and analyzed. Key results are summarized along with further discussion in section 4.

## 2. Model setup and reference datasets

### 2.1. Irrigation scheme

As a state-of-the-art Earth modeling framework, CESM 1.2.0 consists of coupled atmospheric, oceanic, land and sea ice models [Neale *et al.*, 2010b; Hurrell *et al.*, 2013]. In this study, CAM version 5 (CAM5) [Neale *et al.*, 2010b] and CLM version 4.0 [Oleson *et al.*, 2010a] are used. Global sea-surface temperatures are prescribed in accordance with the Atmospheric Model Intercomparison Project (AMIP) protocol [?]. The finest horizontal resolution of our grid is  $\sim 28$  km covering the western U.S., with a quasi-uniform  $1^\circ$  mesh over the remainder of the globe (see Figure 1). Considering the relatively flat topography (less than 100 m) over most of CV, the  $\sim 28$  km grid resolution satisfies our need for modeling irrigation effects. In particular, simulations at  $0.125^\circ$  ( $\sim 14$  km) conducted in ? did not show a statistically significant change in temperature statistics over California. In our study, as in Zarzycki *et al.* [2015], general circulation patterns (e.g., wind, pressure and precipitation) do not exhibit apparent artifacts in the variable-resolution transition region. A detailed description of the techniques of VR-CESM employed in this paper can be found in Rhoades *et al.* [2015]. Here, our model description focuses on the irrigation scheme within CLM 4.0.

The fractional land-use data used for computing cropland (independent of specific type) that is equipped for irrigation within each grid cell is from Siebert *et al.* [2005] for the year 2000, and is fixed over the simulation period (see Figure 2). This assumption is reasonable



138 since irrigated area has been largely unchanged in California since year 1980 [*Bonfils and*  
 139 *Lobell*, 2007].

140 The need for daily irrigation is determined at 6 AM local time by computing the deficit  
 141 between the current soil moisture content and a target soil moisture content [so no in-  
 142 filtration rate is considered for the irrigation scheme]. If positive, the difference is then  
 143 added to the ground surface at a constant rate over the following four hours, bypassing  
 144 canopy interception. By default, CLM simulates ten soil layers, with a total depth of 3.4  
 145 m [no info in the technical note of the specific depth for each layer or the total depth,  
 146 and there is conflict for the number of soil layers.] [*Oleson et al.*, 2010a]. The target soil  
 147 moisture content in each soil layer  $i$  ( $w_{target,i}$ , in kg/m<sup>2</sup>) is a weighted average of (a) the  
 148 minimum soil moisture content that results in no water stress ( $w_{o,i}$ , kg/m<sup>2</sup>) and (b) the  
 149 soil moisture content at saturation ( $w_{sat,i}$ , kg/m<sup>2</sup>), in accordance with

$$w_{target,i} = (1 - \alpha) * w_{o,i} + \alpha * w_{sat,i} \quad (1)$$

150 The default value of the irrigation weight factor  $\alpha$  is 0.7, which was determined empiri-  
 151 cally to give global, annual irrigation amounts that approximately match observed gross  
 152 irrigation water use around the year 2000 [*Shiklomanov*, 2000]. This parameterization is  
 153 designed to approximate human behavior – that is, enough water is added so as to avoid  
 154 water stress in crops, but not so much that the soil is completely saturated. More details  
 155 about the irrigation model can be found in the online technical description [?].

## 2.2. Simulations

In order to understand the impacts on the local climate triggered by irrigation over the CV, we have conducted a control run (NRG) without irrigation and two irrigation-enabled runs, referred to as IRG and IRG(0.5) respectively. The IRG run uses the default irrigation weight factor ( $\alpha = 0.7$ ). This value was adjusted to 0.5 to get the less irrigated IRG(0.5) run so as to determine the impact of changes in total irrigation water. Simulations were performed over the period 1979-01-02 to 2005-12-31 (UTC). For purposes of analysis, 1979 was discarded as a spin-up period to allow adequate time for the land and atmosphere to equilibrate, with initial soil moisture conditions specified from the output of long-term simulations so as to ensure the groundwater aquifer was in equilibrium with the local climatology. The 26-year time period was chosen to provide an adequate sampling of annual variability within computational constraints. A land cover dataset at 3 min ( $\sim 10$  km) grid resolution for year 2000 was used as it provided a realistic fraction of irrigated cropland in each grid cell over the CV when interpolated onto the 28 km grid (see Figure 2).

It turned out that the irrigated water applied in the IRG simulation was  $\sim 2.84$  mm/day in JJA when averaged over the CV, which equates to  $31.7 \text{ km}^3$  total water. Given that no reliable and comprehensive dataset on cropland use and information is even more sparse on irrigation methods, there are no accurate public numbers about the irrigation area and the irrigation water over CV. However, as we aforementioned, in the year 2000, USGS reported that approximately  $42 \text{ km}^3$  of water was used over  $\sim 41,000 \text{ km}^2$  of irrigated area in California. Based on the fractional of cropland that is equipped for irrigation for year 2000 from *Siebert et al.* [2005] as we mentioned in last part, we arrived at the

estimation of the irrigation area of CV of about  $33,190 \text{ km}^2$ , which is about 81% of the total irrigation area. Assuming between half to two thirds of the  $42 \text{ km}^3$  of water was employed over the CV during JJA (excluding certain water amount for late spring and early fall), that resolves to about 21 to  $28 \text{ km}^3$ , or 0.66 to 0.88 times the amount used by IRG ( $\sim 32 \text{ km}^3$ ). These numbers suggest that the water use imposed by this irrigation scheme is fairly realistic.

iiiiii HEAD ===== It turned out that the irrigated water applied in the IRG simulation was  $\sim 2.84 \text{ mm/day}$  in JJA when averaged over the CV, which equates to  $31.7 \text{ km}^3$  total water. Given that no reliable and comprehensive dataset on cropland use and information is even more sparse on irrigation methods, there are no accurate public numbers about the irrigation area and the irrigation water over CV. However, as we aforementioned, in the year 2000, USGS reported that approximately  $42 \text{ km}^3$  of water was used over  $41,000 \text{ km}^2$  of irrigated area in California. Based on the fractional of cropland that is equipped for irrigation for year 2000 from *Siebert et al.* [2005] as we mentioned in last part, we arrived at the estimation of the irrigation area of CV of about  $33,190 \text{ km}^2$ , which is about 81% of the total irrigation area. Assuming between half to two thirds of the  $42 \text{ km}^3$  of water was employed over the CV during JJA (excluding certain water amount for late spring and early fall), that resolves to about 21 to  $28 \text{ km}^3$ , or 0.66 to 0.88 times the amount used by IRG ( $\sim 32 \text{ km}^3$ ). These numbers suggest that the water use imposed by this irrigation scheme is fairly realistic.

LLLLLL origin/master

### 3. Methodology

In the CV, irrigation peaks during the summer growing season [*Salas et al.*, 2006] in response to California’s dry Mediterranean summers (with a precipitation rate of about 0.13 mm/day averaged over year 1980-2005). Our simulations accurately reproduce this observation, as most irrigated water is added during summer (see Figure 1 in the supplement document). To study the climatological impacts of irrigation, we focus primarily on changes in June, July and August (JJA) near-surface (2 m) temperatures including daily maximum, minimum and average temperatures (Tmax, Tmin and Tavg), and the associated mechanisms driving the relative changes.

To determine how irrigation affects heat extremes within the CV, we calculated hot spell length, hot spell frequency, and mean Tmax over the hot spells, based on the JJA daily Tmax over the 1980-2005 period. For our purposes, a hot spell is present in a given grid cell when five or more consecutive days with Tmax exceeds 38°C. This threshold value approximately corresponds to the 90th percentile of all the daily Tmax values within the CV. *Hot spell length* is defined as the average duration (in days) for all hot spells over the 26 year period, *hot spell frequency* is defined as the average number of hot spells per year, and *mean hot spell Tmax* is defined as the average Tmax over all the hot spell days. When analyzing hot spells, declustering is employed following the strategy of *Ferro and Segers* [2003] to ensure hot spells are serially independent. This functionality is implemented in the R package **extRemes** [*Gilleland and Katz*, 2011].

To restrict the analysis to the CV, the variables of interest have been masked and/or averaged within the area defined by the bounded region as sketchily depicted in Figure 2, which contains 155 grid points. To quantify the model performance in comparison with the

reference datasets, the root-mean-square deviation (RMSD) and mean signed difference (MSD) are used, and spatial correlation (Corr) is assessed by computing sample linear cross-correlations at lag 0 after converting a two-dimensional dataset to a one-dimensional array. Mathematically, RMSD and MSD are written as,

$$RMSD = \sqrt{\frac{1}{N} \sum_{i=1}^N (v_i - \hat{v}_i)^2} \quad MSD = \frac{1}{N} \sum_{i=1}^N (v_i - \hat{v}_i) \quad (2)$$

where  $v_i$  and  $\hat{v}_i$  are values from the simulation output and reference dataset respectively;  $i$  is the grid-point index and  $N$  is the total number of grid points over specific regions.

Throughout the remainder of this paper, Student's t-test has been used to test the equality of the means of two datasets. This is employed for the seasonally-averaged data at each grid point and for spatially averaged data over CV. F-test is applied to test whether the sample variances are equal. These tests are used here when the sample population can be adequately described by a normal distribution, where normality is assessed under the Anderson-Darling test. All these tests are evaluated at the  $\alpha = 0.05$  significance level.

### 3.1. Reference datasets

For comparison, we employ two high-quality gridded observational datasets (UW and PRISM) and selected weather station data (NCDC) to evaluate our simulation output. The detailed descriptions of these reference datasets are as follows.

**UW:** The UW daily gridded meteorological data is obtained from the Surface Water Modeling group at the University of Washington [Maurer *et al.*, 2002; Hamlet and Lettenmaier, 2005]. The dataset is provided at  $0.125^\circ$  horizontal resolution covering the period

from year 1949 to 2010 with daily time frequency for Tmax and Tmin in the aspect of temperature, which are used in this study.

**PRISM:** The Parameter-elevation Regressions on Independent Slopes Model (PRISM) [Daly *et al.*, 2008] gridded dataset at 4 km resolution is also employed in this study. This model ingests point measurements and applies a weighted regression scheme that accounts for key factors affecting the local climatology. PRISM is the United States Department of Agriculture’s official climatological dataset. Monthly climatological variables are available for year 1895 through 2015 and daily data for year 1981 to 2015 from the PRISM Climate Group [?]. This study makes use of monthly Tmax, Tmin, Tavg, and daily Tmax.

**NCDC:** Weather station measurements over the CV are obtained from the Global Historical Climate Network (GHCN) and provided by NOAA/NCDC [?]. Weather stations within the study region were chosen from all stations with at least 90% observations of Tmax over all JJA days from 1981 to 2005. A subset of 11 stations were then chosen to provide roughly even spatial coverage of the CV.

#### 4. Results

The average JJA Tmin, Tavg and Tmax over the 1980-2005 period from all simulations and gridded datasets are depicted in Figure 3. Relative to the gridded datasets, NRG has a prominent overestimation of Tmax, with MSD values of  $\sim 0.75$  K and RMSD values of  $\sim 1.7$  K (see Table 1). The cooling effect caused by irrigation is clear in all temperature fields when comparing NRG and IRG results, with all fields exhibiting significant differences over parts of the CV (as hatched in Figure 3). Notably, no statistically significant difference in temperature arises from reducing the irrigation factor from 0.7 to 0.5. Although the IRG

run shows a slight cold bias with an MSD around -0.36 K (which is reduced in IRG(0.5) to around -0.2 K), this effect is limited to the base of the Sierra Nevada and the San Francisco Bay Delta region.

Compared with NRG, the RMSD of Tmax for IRG(0.5) is only reduced by about 20% against PRISM, which appears to be due to the offset effects caused by the non-irrigated grid cells around our study region's boundary. Although Tmin was also reduced by about 0.5 K in IRG over the irrigated area, all three runs still exhibit a warm bias in this field relative to the reference. The net result is that Tavg is overestimated in NRG over the CV, except in regions influenced by the Delta sea breeze, whereas IRG produced a slight cool bias in Tavg after alleviating the overestimation of Tmax in the northern and southern reaches of the CV. The correlation coefficients between simulations and reference datasets are about 0.76 to 0.86, indicating that VR-CESM can capture the overall spatial distributions of temperature. Although NRG and IRG are highly correlated with each other ( $>0.95$ ), this simply implies that the spatial pattern of IRG is quite similar to NRG under spatially consistent cooling. Over non-irrigated areas, the results are essentially identical among all runs, suggesting that temperature modulation is largely a local phenomenon.

As mentioned earlier, the differences between the IRG and IRG(0.5) simulations were not statistically significant, particularly when compared to the differences between IRG and NRG. Therefore, the intrinsic variability (even with some differences in irrigation water amounts) is small for VR-CESM relative to the effect of irrigation. This further testifies that the statistically significant differences between IRG and NRG are due to enabled irrigation instead of random variation. The overall performance of VR-CESM

in modeling regional climate is out of the scope of this study, but has been extensively discussed in [?].

Key variables associated with the irrigation model have been tabulated in Table 2. Tmax, latent heat flux, precipitation and soil moisture are further illustrated in Figure 4. With the relative scarcity of natural precipitation in summer season ( $\sim 0.1$  mm/day), there is a  $\sim 61\%$  increase in latent heat flux after adding  $\sim 2.84$  mm/day irrigated water for IRG over the hot and dry summer period. The main contribution to latent heat flux increase from NRG to IRG is due to ground evaporation (which is about 2.5 times larger), as vegetation evapotranspiration did not differ significantly between NRG ( $\sim 1.1$  mm/day) and IRG ( $\sim 1.25$  mm/day). Therefore, cooling of Tmax is largely due to increased latent heat flux during the daytime caused by evaporation from the surface.

With irrigation enabled, the specific humidity increased by about 12% due to increased evaporation, and sensible heat flux decreased by 13% with lower surface temperatures and a shift of sensible to latent heat flux. The soil moisture averaged over all the surface and subsurface soil layers showed a statistically significant increase ( $\sim 4.4\%$ ) under irrigation. Since variability of the soil moisture is smaller at lower levels compared to upper levels, even a 4.4% change results in a quite significant variation, especially when we consider the first few thin soil layers in CLM 4.0, with the relative enlargement of soil water being larger than 10% for the topmost five layers (reaching  $\sim 52\%$  at the first thin layer).

iiiiiii HEAD We note that the small difference (about 1.4%, but still significant at significance level 0.05) of soil moistures between IRG and IRG(0.5) might suggest that irrigated water does not effectively infiltrate into lower soil layers, given the irrigated water amount of IRG is more than two times of IRG(0.5). We investigated further and



found that the soil water between IRG and IRG(0.5) is significantly different at the ground surface ( $\sim 5\%$  changes) and the bottom layers ( $\sim 1\%$  changes), but not for near-surface and middle levels. It turns out that most of the added water ( $\sim 1.57$  mm/day) from IRG(0.5) to IRG directly led to surface runoff (parameterized by removing surface water after infiltration into the soil) ( $\sim 0.24$  mm/day for IRG(0.5) and  $\sim 1.6$  mm/day for IRG). This creates a lot of irrigation water waste, since the IRG simulates a comparable amount of irrigation demand as actually observed.

Based on the JJA-averaged values of each year in 26 years period, the distributions of four selected variables are depicted in the box and whisker diagram in Figure 4. With irrigation, both the average magnitude and annual variability of Tmax (around  $0.9^\circ\text{C}$ ) are closer to observations. Compared to NRG, the range of Tmax for irrigation runs reduced to  $\sim 3^\circ\text{C}$  from  $\sim 4.5^\circ\text{C}$  with a more concentrated distribution, **suggesting irrigation had a modulating effect on temperature variability (although the differences of variances are not statistically significant)**. The mean latent heat flux almost doubles when irrigation is enabled, however the variance of the distribution (with inter-annual variation of  $\sim 2.7$   $\text{W}/\text{m}^2$  for IRG and  $\sim 3.3$   $\text{W}/\text{m}^2$  for IRG(0.5)) did not substantially differ from NRG (with inter-annual variation of  $\sim 3.7$   $\text{W}/\text{m}^2$ ).

Further, average precipitation did not significantly change among these three runs (under the Mann-Whitney-Wilcoxon test at 0.05 level) together with the observations ( $\sim 0.13$  mm/day for UW and  $\sim 0.14$  mm/day for PRISM), however adding irrigation tended to widen the range of precipitation intensity (significantly different) (with inter-annual variability around 0.12 to 0.13 mm/day for irrigation runs, and about 0.08 mm/day for NRG). This is possibly due to enhanced local convective processes due to irrigation by modifying

the depths of planetary boundary layer, lifting condensation level, and mixing layer as also found by *DeAngelis et al.* [2010]; *Qian et al.* [2013]. We also observe a statistically significant increase in convective available potential energy (CAPE) over irrigated region and part of its surrounding area in our results (see Figure 3 in the supplement). The mean soil moisture significantly increased under irrigation, with the variance of soil moisture decreasing significantly between IRG (about  $1.5 \text{ kg/m}^2$ ) and NRG ( $\sim 2.2 \text{ kg/m}^2$ ), appearing to simply be due to modulation of soil moisture content associated with the irrigation parameterization. ===== With irrigation enabled, the specific humidity increased by about 12% due to increased evaporation, and sensible heat flux decreased by 13% with lower surface temperatures and a shift of sensible to latent heat flux. The soil moisture averaged over all the subsurface soil layers showed a statistically significant increase ( $\sim 4.4\%$ ) under irrigation. Since variability of the soil moisture is smaller at lower levels compared to upper levels, even a 4.4% change results in a quite significant variation, especially when we consider the first few thin soil layers in CLM 4.0, with the relative enlargement of soil water being larger than 10% for the topmost five layers (reaching 52% at the first thin layer).

We note that the small difference (1.4%, still significant at level 0.05) of soil moistures between IRG and IRG(0.5) might suggest that irrigated water does not effectively infiltrate into lower soil layers, given the irrigated water amount of IRG is more than two times of IRG(0.5). We investigated further and found that the soil water between IRG and IRG(0.5) is significantly different at the ground surface ( $\sim 5\%$  changes) and the bottom layers ( $\sim 1\%$  changes), but not for near-surface and middle levels. It turns out that most of the added water ( $\sim 1.57 \text{ mm/day}$ ) from IRG(0.5) to IRG directly led to surface runoff

(parameterized by removing surface water after infiltration into the soil) ( $\sim 0.24$  mm/day for IRG(0.5) and  $\sim 1.6$  mm/day for IRG). This creates a lot of irrigation water waste, since the IRG simulates a comparable amount of irrigation demand as actually observed.

Based on the JJA-averaged values of each year in 26 years period, the distributions of four selected variables are depicted in the box and whisker diagram in Figure 4. With irrigation, both the average magnitude and annual variability of T<sub>max</sub> (around  $0.9^\circ\text{C}$ ) are closer to observations. Compared to NRG, the range of T<sub>max</sub> for irrigation runs reduced to  $\sim 3^\circ\text{C}$  from  $\sim 4.5^\circ\text{C}$  with a less concentrated distribution, suggesting irrigation had a modulating effect on temperature variability (although the differences of variances are not statistically significant). The mean latent heat flux almost doubles when irrigation is enabled, however the variance of the distribution (with inter-annual variation of  $\sim 2.7$   $\text{W}/\text{m}^2$  for IRG and  $\sim 3.3$   $\text{W}/\text{m}^2$  for IRG(0.5)) did not substantially differ from NRG (with inter-annual variation of  $\sim 3.7$   $\text{W}/\text{m}^2$ ).

Average precipitation did not significantly change among these three runs (under the Mann-Whitney-Wilcoxon test at 95% level) together with the observations ( $\sim 0.13$  mm/day for UW and  $\sim 0.14$  mm/day for PRISM), however adding irrigation tended to widen the range of precipitation intensity (significantly different) (with inter-annual variability around 0.12 to 0.13 mm/day for irrigation runs, and about 0.08 mm/day for NRG). This is possibly due to enhanced local convective processes due to irrigation by modifying the depths of planetary boundary layer, lifting condensation level, and mixing layer as also found by *DeAngelis et al.* [2010]; *Qian et al.* [2013]. We also observe a statistically significant increase in convective available potential energy (CAPE) over irrigated region and a little part of its surrounding area in our results (see Figure 3 in the sup-

plement). Although the mean soil moisture significantly increased under irrigation, the variance of soil moisture also decreased significantly between IRG (about  $1.5 \text{ kg/m}^2$ ) and NRG ( $\sim 2.2 \text{ kg/m}^2$ ), appearing to simply be due to modulation of soil moisture content associated with the irrigation parameterization. *origin/master*

As irrigation clearly led to a strong cooling effect for average Tmax over the hot summers of the CV, we further investigated the frequency distribution of Tmax (as depicted in Figure 5) based on all JJA daily values at each CV grid point for all runs and reference datasets including UW, PRISM and 11 weather stations (area weighted using Voronoi diagram). Since PRISM does not provide daily data for the year 1980, we use the time period from year 1981 to 2005 in this calculation. Overall, the NRG run exhibited an obvious warm bias associated with a relatively long forward tail with Tmax approaching  $48^\circ\text{C}$ . This forward tail was also absent from the NCDC weather station data, adding further evidence that it is associated with unrealistically frequent warm temperatures. However, with irrigation enabled there was much closer agreement with UW and PRISM, especially in the upper tail, although a slight cold bias remains. Examining absolute differences, the first four moments of the frequency distribution of Tmax all showed marked improvement under irrigation (Table 3). Under the Kolmogorov-Smirnov (KS) test, compared with UW and PRISM, the spatially averaged JJA Tmax over the CV for the 25 years (resulting in 25 values) was significantly different for NRG at the 90% level, whereas the difference was not significant for IRG or IRG(0.5).

Hot spell features related with heat extremes are tabulated in Table 4 for simulations and the UW dataset (results from PRISM were effectively equivalent to UW). Hot spells were too long and too frequent without irrigation, but once irrigation was enabled, length,

duration and intensity were all closely matched to UW by the model (no significant differences under t-test). Notably, the cooling effect associated with irrigation led to a reduction in length and frequency of hot spells of about 20% and 30%, respectively (both statistically significant at the 0.05 level). The difference in Tmax between IRG and NRG runs when averaged over hot spells, compared with the seasonal average, was approximately halved (but still significant). It appears that irrigation has less impact on the temperature of hot days, compared with average summer days.

iiiiii HEAD Due to the important role the CV plays in agricultural industry, we have also examined the heat stress experienced by crops. As defined by *Teixeira et al.* [2013], heat stress can be quantified by the number of hours per day exceeding 35°C. In our study, heat stress was assessed for days from June 1st to September 30th (JJAS) for NRG and IRG runs. Given only daily outputs of Tmin and Tmax (as opposed to hourly Temperature values), heat stress was obtained using a cosine fit to approximate hourly temperatures. This approach was validated by comparing the number of hours exceeding 35°C from one year of simulation with hourly output against the cosine approximation. Since the observed discrepancy was only about 4%, the cosine approximation was subsequently applied to obtain hourly temperature exceedance over the 26-year study period in the CV. Based on the averaged hourly counts (depicted in Figure 6), it was observed that both the heat stress intensity and frequency were reduced under irrigation, most obviously during mid-July to early September. The average hours per day exceeding 35°C over the JJAS period was 2.352 for NRG and 1.838 for IRG – a ~22% decrease. ===== Due to the important role the CV plays in agricultural industry, we have also examined the heat stress experienced by crops. As defined by *Teixeira et al.* [2013], heat stress

can be quantified by the number of hours per day that exceed 35°C. In our study, heat stress was assessed for days from June 1st to September 30th (JJAS) for NRG and IRG runs. Given only daily outputs of Tmin and Tmax (as opposed to hourly T values), heat stress was obtained using a cosine fit to approximate hourly temperatures. This approach was validated by comparing the tallied number of hours exceeding 35°C from one year of simulation with hourly output against the cosine approximation. Since the observed discrepancy was only about 4%, the cosine approximation was subsequently applied to obtain hourly temperature exceedance over the 26-year study period in the CV. Based on the averaged hourly counts (depicted in Figure 6), it was observed that both the heat stress intensity and frequency were reduced under irrigation, most obviously during mid-July to early September. The average hours per day exceeding 35°C over the JJAS period was 2.352 for NRG and 1.838 for IRG – a  $\sim 22\%$  decrease. *origin/master*

## 5. Discussion and Summary

With irrigation employed, nighttime warming is expected to occur, leading to an increase in daily Tmin due to the increased thermal conductivity of wet soil, as found by *Kanamaru and Kanamitsu* [2008]. However, in our irrigation-enabled runs, Tmin did not increase but instead decreased over part of the irrigated area (statistically significant, although the magnitude of this decrease was much smaller than that of Tmax). As thoroughly argued by *Bonfils and Lobell* [2007], our result further supports that irrigation does not completely explain the large nighttime warming observed in California. As discussed in *Kueppers et al.* [2008]; *Kanamaru and Kanamitsu* [2008], the sign of the change in Tmin by irrigation practices depends on the irrigation parameterization and the assessed climate model, which might be due to the discrepancy in soil properties with their effects on soil

heat capacity and conductivity, and on the nighttime soilair temperature gradient. This study verifies the findings of previous studies that irrigation generally lowers temperatures in the CV region, but with a smaller magnitude ( $\sim 1.1$  K) compared to what was found by *Lobell et al.* [2006].

*Lo and Famiglietti* [2013] stated that increases in evapotranspiration and water vapor export caused by irrigation significantly impacts the atmospheric circulation in the southwestern United States, including strengthening the regional hydrological cycle, using coupled CAM 3.5 and CLM 3.5 at the grid resolution of  $1.4^\circ$ . However, in our study, no further evidence is observed for an enhanced hydrological cycle and associated increase in water vapor transport as argued by *Lo and Famiglietti* [2013]. There are no significant changes at 90% level (same level as *Lo and Famiglietti* [2013] used) to precipitation, low-level cloud, near-surface specific humidity and CAPE over the southwestern regions (see Figure 3 in the supplement) where *Lo and Famiglietti* [2013] found the remote impacts of irrigation in California’s Central Valley. We do see that there are certain positive increases of precipitation, low-level cloud and CAPE between IRG and NRG over some regions of Nevada and Utah, but not really between IRG(0.5) and NRG. This could be due to the higher increase of soil moisture for IRG compared to NRG. It might suggest that if keeping increase the soil moisture to certain high enough level, the irrigated region could result in notable improvement of the water vapor transport to the downwind region over long-term climate.

HEAD We have also explored the possible mechanisms by which irrigation may bring about global changes, including the latent heat flux, near-surface specific humidity, precipitation and cloud cover globally. The quantitative impacts are quite similar to what

has been obtained in *Sacks et al.* [2009], thus not shown here. In order to see if applying the irrigation changes the overall atmosphere circulation, the geopotential heights at 500 hPa (see Figure 2 in supplement) for all simulations show similar patterns with only a few regions with significant differences. Since no clear pattern was present in those regions among the simulations, and there is no clear physical mechanism to connect these regions with irrigated regions, we attribute these differences to insufficient ensemble size.

===== We have also explored the possible mechanisms by which irrigation may bring about global changes, including the latent heat flux, near-surface specific humidity, precipitation and cloud cover globally. The quantitative impacts are quite similar to what has been shown in *Sacks et al.* [2009]. The geopotential heights at 500 hPa (see Figure 2 in supplement) for all simulations show similar patterns with only a few regions with significant difference. Since no clear pattern was present in regions with statistically significant differences (among NRG, IRG(0.5) and IRG), and there is no clear physical mechanism to connect these regions with irrigated regions, we attribute these differences to insufficient ensemble size.

By decreasing the irrigation weight from 0.7 to 0.5, total irrigated water employed has reduced by half. Nonetheless, the climatological impacts observed in IRG(0.5) were quite similar to IRG. To understand the climatological impacts under an extreme water deficit, we also performed a five year test run where the irrigation weight factor was set to zero, and added half of the water that was calculated from the deficit equation described in Section 2, resulting in irrigated water being applied at 0.42 mm/day. In this case, the average latent heat flux was around 50.65 W/m<sup>2</sup>, which is about 80% of the value of IRG run. This emphasizes the non-linear dependency between irrigated water application and resultant



latent heat flux: specifically, most of the extra water applied in the irrigation calculation simply resulted in surface runoff rather than an enhancement of soil moisture, suggesting that CLM performs relatively conservatively in soil moisture regulation. According to the technical report of the CLM 4.0 by *Oleson et al.* [2010a], the maximum infiltration capacity is determined from soil texture and soil moisture [?] and the runoff is parameterized by the simple TOPMODEL-based [?] runoff model (SIMTOP) described by ?. In CLM 4.0 *Oleson et al.* [2010a], the surface and subsurface runoff simply goes to nearby river and then end up in ocean routed in the river route model (RTM). In our simulations, RTM is not enabled, since it lacks realistic control of water infiltration or groundwater replenishment as a watershed model. We hypothesize that a coupled system with an integrated hydrological modeling system is necessary to correctly represent the regional hydrological processes. ~~~~~~~~~ origin/master

By decreasing the irrigation weight from 0.7 to 0.5, total irrigated water employed has nearly reduced by half. Nonetheless, the climatological impacts observed in IRG(0.5) were quite similar to IRG. To understand the climatological impacts under an extreme water deficit, we also performed a five year test run in which the irrigation weight factor was set to zero, and added half of the water that was calculated from the deficit equation described in Section 2, resulting in irrigated water being applied at 0.42 mm/day. In this case, the average latent heat flux was around 50.65 W/m<sup>2</sup>, which is about 80% of the value of IRG run. This emphasizes the non-linear dependency between irrigated water application and resultant latent heat flux: specifically, most of the extra water applied in the irrigation calculation simply resulted in surface runoff rather than an enhancement of soil moisture, suggesting that CLM performs relatively conservatively in soil moisture

regulation. According to the technical report of the CLM 4.0 [Oleson *et al.*, 2010a], the maximum infiltration capacity is determined from soil texture and soil moisture [?] and the runoff is parameterized by the simple TOPMODEL-based [?] runoff model (SIMTOP) described by ?. In CLM 4.0, the surface and subsurface runoff simply goes to nearby river and then end up in ocean routed in the river route model (RTM). In our simulations, RTM is not enabled, since it lacks realistic control of water infiltration or groundwater replenishment as a watershed model. We hypothesize that a coupled system with an integrated hydrological modeling system is necessary to correctly represent the regional hydrological processes.

To summarize, the variable-resolution Community Earth System Model (VR-CESM) was used to simulate the impact of irrigation on the regional climate of California’s Central Valley (CV), one of the most heavily irrigated and productive areas in the U.S. Within the land component model (i.e. CLM), an irrigation scheme with relatively realistic estimates of water use was employed. The cooling effect caused by irrigation was obvious in the Tmax field with a magnitude around 1.1 K (seasonally averaged over summer months), which arose from the greatly increased ( $\sim 61\%$ ) latent heat flux associated with daytime ground evaporation. With irrigation, both the average magnitude and annual variability of Tmax were better captured when compared with gridded observations and weather station data. Compared with Tmax, smaller differences were observed for Tmin over the irrigated area, but no statistically significant impacts from irrigation were observed over the surrounding non-irrigated area’s climate. Although irrigated water did not effectively infiltrate into lower soil layers, soil moisture nonetheless exhibited a statistically significant increase (with a slight amplitude  $\sim 4.4\%$ ) under heavy irrigation. With irrigation enabled,

an exceptional warm bias associated with a long forward tail of the frequency distribution of  $T_{\max}$  is alleviated, although a slight cold bias remained at higher elevations. Further, the cooling effect associated with irrigation led to a reduction in length and frequency of hot spells for about 20% and 30%, closely matched to observations, and a decrease in the heat stress frequency by about 22% for cropland. This work suggests that the irrigation scheme should be enabled for regional climate studies with CLM and CESM, particularly over heavily irrigated regions.

In this study, we have argued that irrigation in the CV is an important component of the region's surface energy budget that must be parameterized in high-resolution climate models in order to properly simulate temperature statistics. The ongoing California drought (2012-present) highlights the importance of water resources to agriculture in the CV. In the absence of surface water for irrigation, groundwater reserves were depleted in order to maintain agricultural production. However, it is widely acknowledged that in a prolonged future drought, continued groundwater pumping would not be sustainable, which would in turn lead to a reduction in applied irrigation water [maybe shorten a little bit]. This study suggests that under these conditions, warming from climate change, which is tampered by irrigation in the CV, would be exacerbated and leads to a substantial increase in daily  $T_{\max}$  throughout the CV with repercussions for human health and heat stress [Williams *et al.*, 2015]. Consequently, we anticipate this study can be extended to better understanding the feedbacks associated with prolonged drought conditions in the U.S. West.

## Acknowledgments.

The authors would like to thank Dr. Travis O’Brien and Dr. Richard Grotjahn for many useful suggestions. We would also like to thank IT support for our local UC Davis computing cluster. We acknowledge the substantial effort behind the datasets used in this study, including PRISM, UW and NCDC. The simulation data used is available by request at xyhuang@ucdavis.edu. This project is supported in part by the University of California, Davis and by the Department of Energy “Multiscale Methods for Accurate, Efficient, and Scale-Aware Models of the Earth System” project. Support also comes from the California Agricultural Experiment Station (project CA-D-LAW-2203-H).

## References

- Adegoke, J. O., R. A. Pielke Sr, J. Eastman, R. Mahmood, and K. G. Hubbard (2003), Impact of irrigation on midsummer surface fluxes and temperature under dry synoptic conditions: A regional atmospheric model study of the us high plains, *Monthly Weather Review*, *131*(3), 556–564.
- Bonan, G. B. (1997), Effects of land use on the climate of the united states, *Climatic Change*, *37*(3), 449–486.
- Bonfils, C., and D. Lobell (2007), Empirical evidence for a recent slowdown in irrigation-induced cooling, *Proceedings of the National Academy of Sciences*, *104*(34), 13,582–13,587.
- Boucher, O., G. Myhre, and A. Myhre (2004), Direct human influence of irrigation on atmospheric water vapour and climate, *Climate Dynamics*, *22*(6-7), 597–603.
- Daly, C., M. Halbleib, J. I. Smith, W. P. Gibson, M. K. Doggett, G. H. Taylor, J. Curtis, and P. P. Pasteris (2008), Physiographically sensitive mapping of climatological temper-

- 579 ature and precipitation across the conterminous United States, *International Journal*  
580 *of Climatology*, 28(15), 2031–2064.
- 581 DeAngelis, A., F. Dominguez, Y. Fan, A. Robock, M. D. Kustu, and D. Robinson (2010),  
582 Evidence of enhanced precipitation due to irrigation over the great plains of the united  
583 states, *Journal of Geophysical Research: Atmospheres (1984–2012)*, 115(D15).
- 584 Döll, P., and S. Siebert (2002), Global modeling of irrigation water requirements, *Water*  
585 *Resources Research*, 38(4), 8–1.
- 586 Famiglietti, J., M. Lo, S. Ho, J. Bethune, K. Anderson, T. Syed, S. Swenson, C. de Linage,  
587 and M. Rodell (2011), Satellites measure recent rates of groundwater depletion in cali-  
588 fornia’s central valley, *Geophysical Research Letters*, 38(3).
- 589 Ferro, C. A., and J. Segers (2003), Inference for clusters of extreme values, *Journal of the*  
590 *Royal Statistical Society: Series B (Statistical Methodology)*, 65(2), 545–556.
- 591 Foley, J. A., M. H. Costa, C. Delire, N. Ramankutty, and P. Snyder (2003), Green surprise?  
592 how terrestrial ecosystems could affect earth’s climate, *Frontiers in Ecology and the*  
593 *Environment*, 1(1), 38–44.
- 594 Fox-Rabinovitz, M. S., G. L. Stenchikov, M. J. Suarez, and L. L. Takacs (1997), A  
595 finite-difference GCM dynamical core with a variable-resolution stretched grid, *Monthly*  
596 *Weather Review*, 125(11), 2943–2968.
- 597 Gilleland, E., and R. W. Katz (2011), New software to analyze how extremes change over  
598 time, *Eos, Transactions American Geophysical Union*, 92(2), 13–14.
- 599 Hamlet, A. F., and D. P. Lettenmaier (2005), Production of Temporally Consistent Grid-  
600 ded Precipitation and Temperature Fields for the Continental United States\*, *Journal*  
601 *of Hydrometeorology*, 6(3), 330–336.

- Hurrell, J. W., M. M. Holland, P. R. Gent, S. Ghan, J. E. Kay, P. Kushner, J.-F. Lamarque, W. G. Large, D. Lawrence, K. Lindsay, et al. (2013), The community earth system model: A framework for collaborative research, *Bulletin of the American Meteorological Society*, *94*(9), 1339–1360.
- Kanamaru, H., and M. Kanamitsu (2008), Model diagnosis of nighttime minimum temperature warming during summer due to irrigation in the california central valley, *Journal of Hydrometeorology*, *9*(5), 1061–1072.
- Kueppers, L. M., M. A. Snyder, and L. C. Sloan (2007), Irrigation cooling effect: Regional climate forcing by land-use change, *Geophysical Research Letters*, *34*(3).
- Kueppers, L. M., M. A. Snyder, L. C. Sloan, D. Cayan, J. Jin, H. Kanamaru, M. Kanamitsu, N. L. Miller, M. Tyree, H. Du, et al. (2008), Seasonal temperature responses to land-use change in the western united states, *Global and Planetary Change*, *60*(3), 250–264.
- Laprise, R., R. De Elia, D. Caya, S. Biner, P. Lucas-Picher, E. Diaconescu, M. Leduc, A. Alexandru, and L. Separovic (2008), Challenging some tenets of regional climate modelling, *Meteorology and Atmospheric Physics*, *100*(1-4), 3–22.
- Leng, G., M. Huang, Q. Tang, W. J. Sacks, H. Lei, and L. R. Leung (2013), Modeling the effects of irrigation on land surface fluxes and states over the conterminous united states: Sensitivity to input data and model parameters, *Journal of Geophysical Research: Atmospheres*, *118*(17), 9789–9803.
- Leung, L. R., L. O. Mearns, F. Giorgi, and R. L. Wilby (2003), Regional climate research: needs and opportunities, *Bulletin of the American Meteorological Society*, *84*(1), 89–95.

- Lo, M.-H., and J. S. Famiglietti (2013), Irrigation in california’s central valley strengthens the southwestern us water cycle, *Geophysical Research Letters*, *40*(2), 301–306.
- Lobell, D., G. Bala, and P. Duffy (2006), Biogeophysical impacts of cropland management changes on climate, *Geophysical Research Letters*, *33*(6).
- Lobell, D. B., and C. Bonfils (2008), The effect of irrigation on regional temperatures: A spatial and temporal analysis of trends in california, 1934-2002, *Journal of Climate*, *21*(10), 2063–2071.
- Lobell, D. B., C. J. Bonfils, L. M. Kueppers, and M. A. Snyder (2008), Irrigation cooling effect on temperature and heat index extremes, *Geophysical Research Letters*, *35*(9).
- Mahmood, R., S. A. Foster, T. Keeling, K. G. Hubbard, C. Carlson, and R. Leeper (2006), Impacts of irrigation on 20th century temperature in the northern great plains, *Global and Planetary Change*, *54*(1), 1–18.
- Maurer, E., A. Wood, J. Adam, D. Lettenmaier, and B. Nijssen (2002), A long-term hydrologically based dataset of land surface fluxes and states for the conterminous United States\*, *Journal of climate*, *15*(22), 3237–3251.
- Neale, R. B., C.-C. Chen, A. Gettelman, P. H. Lauritzen, S. Park, D. L. Williamson, A. J. Conley, R. Garcia, D. Kinnison, J.-F. Lamarque, et al. (2010a), Description of the NCAR community atmosphere model (CAM 5.0), *NCAR Tech. Note NCAR/TN-486+STR*.
- Neale, R. B., C.-C. Chen, A. Gettelman, P. H. Lauritzen, S. Park, D. L. Williamson, A. J. Conley, R. Garcia, D. Kinnison, J.-F. Lamarque, D. Marsh, M. Mills, A. K. Smith, S. Tilmes, F. Vitt, P. Cameron-Smith, W. D. Collins, M. J. Iacono, , R. C. Easter, X. Liu, S. J. Ghan, P. J. Rasch, and M. A. Taylor (2010b), Description of the

- 647 NCAR Community Atmosphere Model (CAM 5.0), *NCAR Technical Note NCAR/TN-*  
648 *486+STR*, National Center for Atmospheric Research, Boulder, Colorado.
- 649 Oleson, K., D. Lawrence, G. Bonan, M. Flanner, E. Kluzek, P. Lawrence, S. Levis,  
650 S. Swenson, P. Thornton, A. Dai, M. Decker, R. Dickinson, J. Feddema, C. Heald,  
651 F. Hoffman, J. Lamarque, N. Mahowald, G. Niu, T. Qian, J. Randerson, S. Running,  
652 K. Sakaguchi, A. Slater, R. Stockli, A. Wang, Z. Yang, X. Zeng, and X. Zeng (2010a),  
653 Technical description of version 4.0 of the Community Land Model (CLM), *NCAR Tech-*  
654 *nical Note NCAR/TN-478+STR*, National Center for Atmospheric Research, Boulder,  
655 Colorado, doi:10.5065/D6FB50WZ.
- 656 Oleson, K. W., D. M. Lawrence, B. Gordon, M. G. Flanner, E. Kluzek, J. Peter, S. Levis,  
657 S. C. Swenson, E. Thornton, J. Feddema, et al. (2010b), Technical description of version  
658 4.0 of the community land model (clm).
- 659 Pielke, R. A., G. Marland, R. A. Betts, T. N. Chase, J. L. Eastman, J. O. Niles, S. W.  
660 Running, et al. (2002), The influence of land-use change and landscape dynamics on  
661 the climate system: relevance to climate-change policy beyond the radiative effect of  
662 greenhouse gases, *Philosophical Transactions of the Royal Society of London A: Math-*  
663 *ematical, Physical and Engineering Sciences*, 360(1797), 1705–1719.
- 664 Qian, Y., M. Huang, B. Yang, and L. K. Berg (2013), A modeling study of irrigation  
665 effects on surface fluxes and land–air–cloud interactions in the southern great plains,  
666 *Journal of Hydrometeorology*, 14(3), 700–721.
- 667 Rauscher, S. A., E. Coppola, C. Piani, and F. Giorgi (2010), Resolution effects on regional  
668 climate model simulations of seasonal precipitation over Europe, *Climate Dynamics*,  
669 35(4), 685–711.



- 670 Rhoades, A. M., X. Huang, P. A. Ullrich, and C. M. Zarzycki (2015), Characterizing  
671 sierra nevada snowpack using variable-resolution cesm, *Journal of Applied Meteorology*  
672 *and Climatology*, (2015).
- 673 Sacks, W. J., B. I. Cook, N. Buening, S. Levis, and J. H. Helkowski (2009), Effects of  
674 global irrigation on the near-surface climate, *Climate Dynamics*, *33*(2-3), 159–175.
- 675 Salas, W., P. Green, S. Froking, and C. Li (2006), Estimating irrigation water use for  
676 california agriculture: 1950s to present, *Contract*, *603*, 862–0244.
- 677 Segal, M., Z. Pan, R. Turner, and E. Takle (1998), On the potential impact of irrigated  
678 areas in north america on summer rainfall caused by large-scale systems, *Journal of*  
679 *Applied Meteorology*, *37*(3), 325–331.
- 680 Shiklomanov, I. A. (2000), Appraisal and assessment of world water resources, *Water*  
681 *international*, *25*(1), 11–32.
- 682 Siebert, S., P. Döll, J. Hoogeveen, J.-M. Faures, K. Frenken, and S. Feick (2005), Develop-  
683 ment and validation of the global map of irrigation areas, *Hydrology and Earth System*  
684 *Sciences Discussions Discussions*, *2*(4), 1299–1327.
- 685 Siebert, S., P. Döll, S. Feick, J. Hoogeveen, and K. Frenken (2007), *Global Map of Irriga-*  
686 *tion Areas*, FAO Frankfurt, Germany.
- 687 Snyder, M., L. Kueppers, L. Sloan, D. Cavan, J. Jin, H. Kanamaru, N. Miller, M. Tyree,  
688 H. Du, and B. Weare (2006), Regional climate effects of irrigation and urbanization  
689 in the western united states: A model intercomparison, *Lawrence Berkeley National*  
690 *Laboratory*.
- 691 Solomon, S. (2007), *Climate change 2007-the physical science basis: Working group I*  
692 *contribution to the fourth assessment report of the IPCC*, vol. 4, Cambridge University

Press.

Staniforth, A. N., and H. L. Mitchell (1978), A variable-resolution finite-element technique for regional forecasting with the primitive equations, *Monthly Weather Review*, *106*(4), 439–447.

Teixeira, E. I., G. Fischer, H. van Velthuisen, C. Walter, and F. Ewert (2013), Global hot-spots of heat stress on agricultural crops due to climate change, *Agricultural and Forest Meteorology*, *170*, 206–215.

Wilkinson, R., K. Clarke, J. Reichman, and J. Dozier (2002), Preparing for a changing climate: the potential consequences of climate variability and change for california, *Report for the US Global Change Research Program*.

Williams, A. P., R. Seager, J. T. Abatzoglou, B. I. Cook, J. E. Smerdon, and E. R. Cook (2015), Contribution of anthropogenic warming to california drought during 2012–2014, *Geophysical Research Letters*.

Zarzycki, C. M., C. Jablonowski, D. R. Thatcher, and M. A. Taylor (2015), Effects of localized grid refinement on the general circulation and climatology in the community atmosphere model, *Journal of Climate*, *28*(7), 2777–2803.

**Table 1.** RMSD ( $^{\circ}\text{C}$ ), MSD ( $^{\circ}\text{C}$ ) (left column minus top row) and Corr of Tmax, Tmin and Tavg between models and gridded observations over the CV in JJA (1980-2005).

<b>JJA Tmax</b>	UW			PRISM			NRG		
	RMSD	MSD	Corr	RMSD	MSD	Corr	RMSD	MSD	Corr
<b>NRG</b>	1.685	0.749	0.857	1.689	0.751	0.856			
<b>IRG</b>	1.511	-0.357	0.816	1.422	-0.355	0.841	1.378	-1.105	0.973
<b>IRG(0.5)</b>	1.467	-0.205	0.821	1.383	-0.203	0.843	1.251	-0.953	0.975
<b>JJA Tmin</b>	UW			PRISM			NRG		
	RMSD	MSD	Corr	RMSD	MSD	Corr	RMSD	MSD	Corr
<b>NRG</b>	2.929	2.117	0.799	2.759	1.596	0.763			
<b>IRG</b>	2.505	1.694	0.797	2.272	1.173	0.774	0.659	-0.423	0.993
<b>IRG(0.5)</b>	2.536	1.730	0.797	2.306	1.209	0.773	0.625	-0.387	0.993
<b>JJA Tavg</b>	PRISM			NRG					
	RMSD	MSD	Corr	RMSD	MSD	Corr	RMSD	MSD	Corr
<b>NRG</b>	1.746	0.478	0.851						
<b>IRG</b>	1.340	-0.309	0.862			1.066	-0.786	0.983	
<b>IRG(0.5)</b>	1.318	-0.215	0.863			0.992	-0.692	0.984	

**Table 2.** Key variables associated with irrigation within the CV in JJA (1980-2005).

	Irrigated water (mm/day)	Latent heat flux (W/m <sup>2</sup> )	Sensible heat flux (W/m <sup>2</sup> )	Ground evaporation (mm/day)	Surface runoff (mm/day)	Soil moisture (kg/m <sup>2</sup> )	Precipitation (mm/day)	2m specific humidity (g/kg)
<b>NRG</b>	0.000	38.832	120.458	0.257	0.016	114.114	0.101	6.989
<b>IRG</b>	2.838	62.574	104.752	0.907	1.610	119.158	0.119	7.852
<b>IRG(0.5)</b>	1.272	61.695	105.730	0.892	0.236	117.550	0.118	7.782

**Table 3.** The first four moments of the JJA Tmax frequency for models and observations over CV. Column titles refer to the Average (Avg), Variance (Var), Skewness (Skew) and Kurtosis (Kurt).

	Avg	Var	Skew	Kurt
<b>NRG</b>	33.535	25.732	-0.445	0.252
<b>IRG</b>	32.374	21.343	-0.505	0.415
<b>IRG(0.5)</b>	32.537	21.125	-0.556	0.632
<b>UW</b>	32.745	22.442	-0.717	0.794
<b>PRISM</b>	32.814	24.007	-0.802	1.120

**Notes:** If skew  $> 0$  [skew  $< 0$ ], the distribution trails off to the right [left]. If kurtosis  $> 0$  [ $< 0$ ], a sharper [flatter] peak compared to a normal distribution (leptokurtic and platykurtic, respectively) is expected.

**Table 4.** Hot spell features including length (days), number and mean Tmax ( $^{\circ}\text{C}$ ) from simulations and UW data over the CV in JJA from 1980-2005.

	NRG	IRG	IRG(0.5)	UW
<b>Hot spell length</b>	8.810	7.014	6.483	6.930
<b>Hot spell number</b>	2.174	1.500	1.505	1.539
<b>Hot spell Tmax</b>	40.340	39.806	39.887	39.720



**Figure 1.** (a) The approximate grid spacing used for the VR-CESM  $0.25^\circ$  mesh. (b) A depiction of the transition from the global  $1^\circ$  resolution mesh through two layers of refinement to  $0.25^\circ$ .



**Figure 2.** The percent of irrigated cropland at each grid cell. The black line delineates the boundary of the CV region.



**Figure 3.** Average JJA Tmax, Tmin and Tavg over year 1980-2005 for models and observations ( $^{\circ}\text{C}$ ). Hatching denotes statistically significant differences between NRG and IRG.

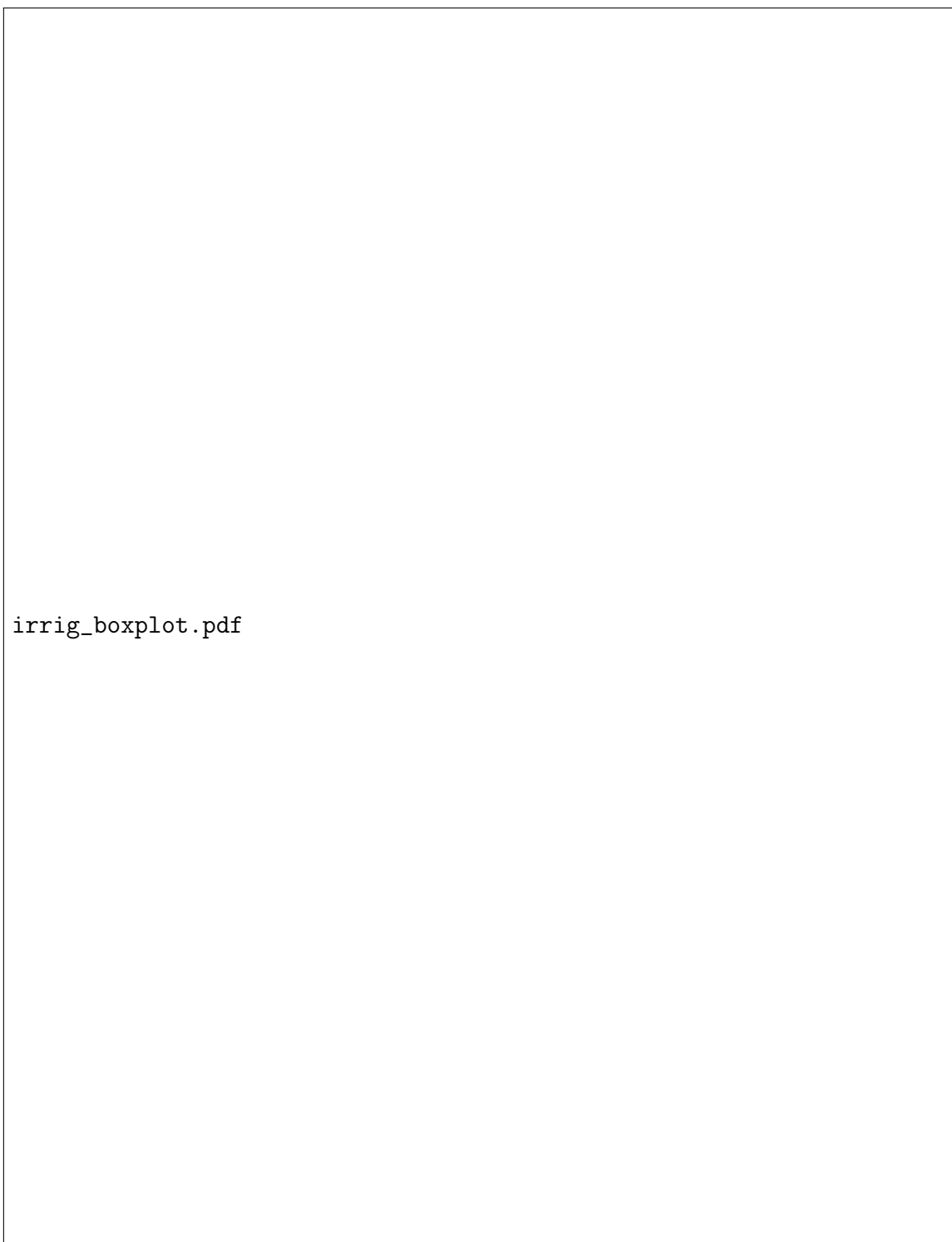


**Figure 4.** Box plots for JJA averaged (a) Tmax, (b) Latent heat flux, (c) Precipitation, and (d) Soil moisture. From top to bottom, horizontal lines represent maximum value, third quartile, median, first quartile and minimum value, respectively.



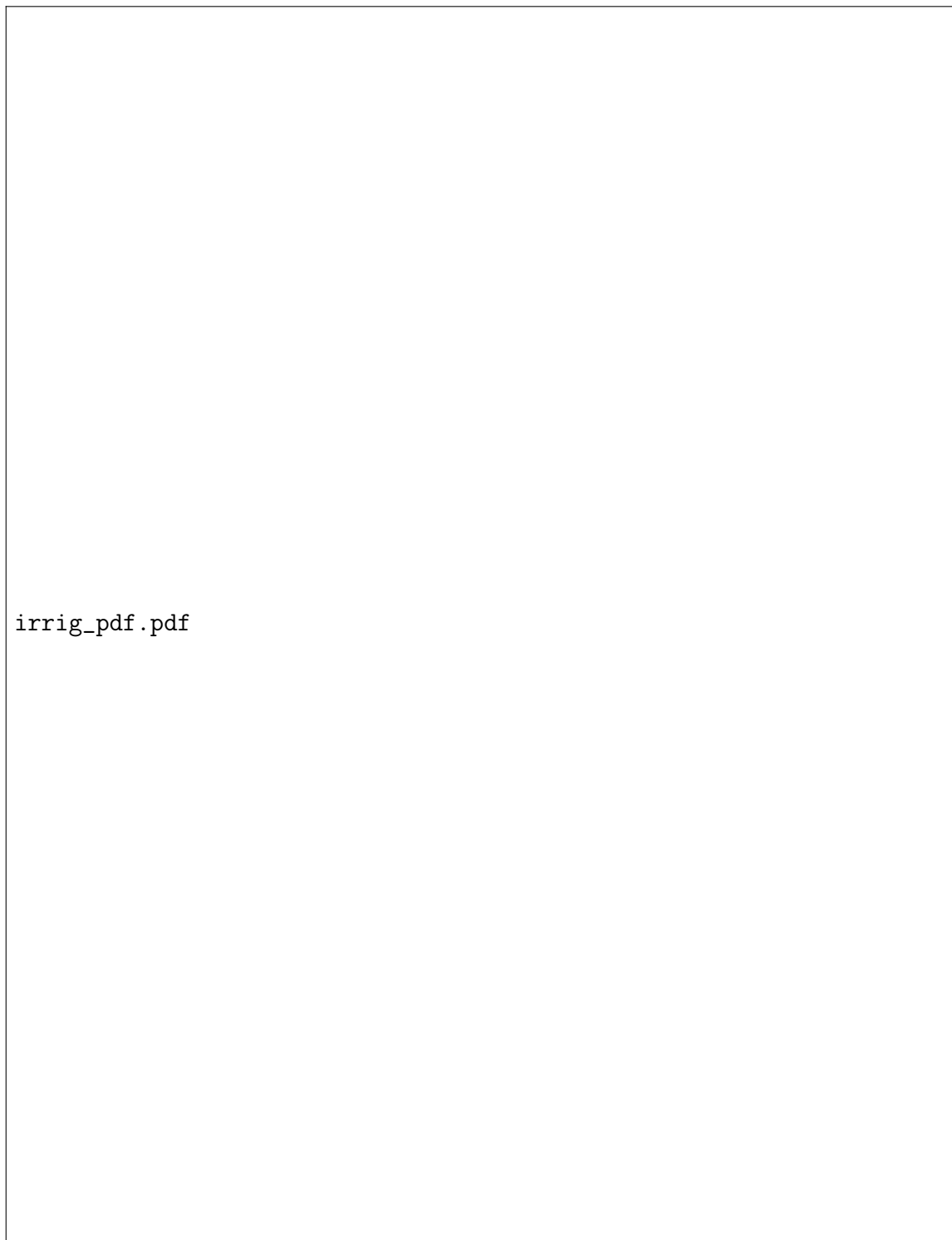


**Figure 5.** Frequency distribution of JJA daily Tmax over the period 1981-2005 from simulations and reference datasets.

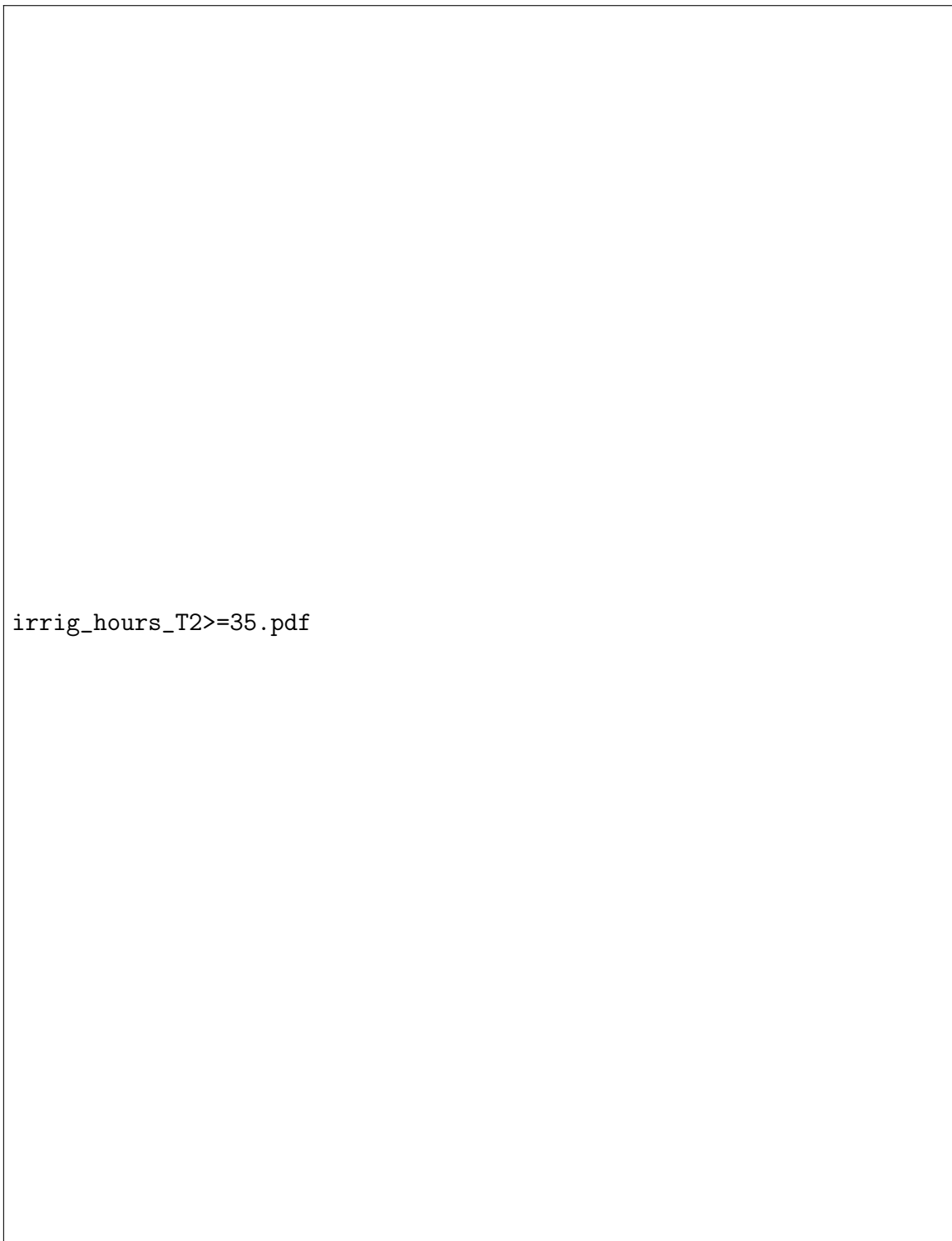


**Figure 6.** The number of hours larger than or equal to  $35^{\circ}\text{C}$  per day from June 1st to September 30th averaged over 1980-2005, for NRG and IRG runs.